(11) F. A. Cotton, B. A. Frenz, J. R. Ebner, and R. A. Walton, *J.C.S. Chem. Commun.*, 4 (1974).
(12) R. S. Nicholson, *Anal. Chem.*, **37**, 1351 (1965).
(13) M. J. Bennett, W. K. Bratton, F. A. Cotton, and W. R. Robinson, *Inorg. Chem.*, **7**, 1570 (1968).
(14) B. R. McGarvey, *Transition Metal Chem.*, **3**, 89 (1966).
(15) F. A. Cotton and C. B. Harris, *Inorg. Chem.*, **6**, 924 (1967).
(16) J. G. Norman and H. J. Kolari, *J. Chem. Soc., Chem. Commun.*, 303 (1974).
(17) P. N. Schatz, University of Virginia, private communication.
(18) C. D. Cowman and H. B. Gray, *J. Amer. Chem. Soc.*, **95**, 8177 (1973).
(19) R. F. Fenske, T. Block, and D. Lichtenberger, unpublished results.

Reactions of Monatomic and Diatomic Manganese with Carbon Monoxide. Matrix Infrared Spectroscopic Evidence for Pentacarbonylmanganese $Mn(CO)_5$ and the Binuclear Carbonyls $Mn_2(CO)_n$ (where $n = 1$ or 2)

H. Huber, E. P. Kündig, G. A. Ozin,* and A. J. Poë

Contributions from the Lash Miller Chemistry Laboratory and Erindale College, University of Toronto, Toronto, Ontario, Canada. *Received June 14, 1974*

Abstract: The reactions of Mn atoms with $^{12}C^{16}O$ and $^{12}C^{16}O$-Ar mixtures at 10–15°K are investigated by matrix isolation infrared spectroscopy and establish the existence of pentacarbonylmanganese, $Mn(CO)_5$, having a C_{4v} square pyramidal stereochemistry. Cotton–Kraihanzel force constants are calculated for $Mn(CO)_5$ and the absorption intensities of the CO stretching modes are used to evaluate the C_{apical}–Mn–C_{eq} angle and the ratio of the axial to equatorial transition dipole moments. The spectral and bonding properties of 15-, 16-, 17-, and 18-electron valence shell pentacarbonyls are reappraised, the $Cr(CO)_5$ problem is clarified, and a simple theory is presented which rationalizes the observed stereochemical changes. Besides its reactions in the monatomic form, manganese is also shown to react as Mn_2 dimers, formed as a result of a surface diffusion effect occurring in the quasi-liquid phase during matrix deposition. The relative concentrations of mononuclear and binuclear species depend on the concentration of metal in the matrix and on the CO:Ar ratios. Using low $^{12}C^{16}O$-Ar ratios which favor Mn_2 formation, the binuclear bridged carbonyl species $Mn_2(CO)_n$ have been synthesised. Mixed $^{12}C^{16}O$-$^{12}C^{18}O$-Ar isotope experiments establish the binuclear complexes to be bridge bonded $Mn_2(CO_b)$ and $Mn_2(CO_b)_2$ and terminally bonded $Mn_2(CO_t)$ and Cotton–Kraihanzel force constants are calculated for all species. The structure and bonding of the binuclear species and their relevance to the chemisorption of CO on manganese metal films are briefly discussed.

Cocondensation reactions of transition metal atoms with small gaseous molecules at low temperatures have recently been shown to provide synthetic routes to a number of chemically interesting species which would have previously been regarded as inaccessible through conventional forms of chemical synthesis. Using these methods, species such as $Ni(N_2)_4$,[1] $Co(CO)_4$,[2] $Ni(CS)_4$,[3] $Ni(CO)_2(N_2)_2$,[4] $Pt(O_2)_2$,[5] $Pt(N_2)_3$,[6] and $Pd(N_2)_2(O_2)$[7] have been synthesised and characterized using matrix infrared and Raman methods of analysis. In most of the cocondensation reactions so far studied, the metals Ni, Pd, and Pt have received greatest attention. These are metals whose ground state atoms have no obvious tendency toward dimerization, as shown by mass spectrometric evidence[8] which establishes at least 99% monatomic metal species in the vapor above the liquid metals, and the formation of mainly *mononuclear* complexes in their matrix reactions.[9]

Recent experiments, however, with V, Cr, Mn, Co, and Cu vapors have led us to believe that under matrix cocondensation conditions, these metals can be induced to form binuclear species. In this paper we report data for the reactions of manganese vapor with carbon monoxide.

Pentacarbonylmanganese, $Mn(CO)_5$. In 1966, Bidinosti and McIntyre discovered that the pyrolysis of $Mn_2(CO)_{10}$ vapor produced appreciable concentrations of the radical $Mn(CO)_5$, detected by its mass spectrum.[10] $Mn(CO)_5^+$ was detected both from low temperature and from high temperature $Mn_2(CO)_{10}$ vaporization. The appearance potential was lower from the high temperature vapor and it was inferred that it was being produced from $Mn(CO)_5$ radicals. It could, in principle, have been formed from any excited form of $Mn_2(CO)_{10}$. A number of studies since then have proposed that it exists as an intermediate in a number of chemical reactions of $Mn_2(CO)_{10}$. Poë, *et al.*,[11] have recently suggested that the kinetics of the thermal decomposition and the reaction of oxygen with $Mn_2(CO)_{10}$ in inert solvents imply that the rate-determining step is homolytic fission of the Mn-Mn bond. Furthermore, Haines and Poë[12] have analyzed kinetic data of Bamford, *et al.*,[13] for vinyl polymerization by mixtures of $Mn_2(CO)_{10}$ and CCl_4, in terms of initiation by CCl_3 radicals produced by the reaction of $Mn(CO)_5$ radicals with CCl_4. The reaction of Br_2 with $Mn_2(CO)_{10}$ in $CHCl_3$ or cyclohexane[14] appears to proceed by a long chain reaction that is believed to involve the propagating reaction

$$Br + Mn_2(CO)_{10} \longrightarrow BrMn(CO)_5 + Mn(CO)_5$$

$$Br_2 + Mn(CO)_5 \longrightarrow Br + BrMn(CO)_5$$

At about the same time, Wiles, *et al.*,[15] produced evidence for the existence of $Mn(CO)_5$ formed in nuclear recoil reactions of ^{56}Mn with solid $Mn_2(CO)_{10}$. The recoiling ^{56}Mn atom was stabilized in the $Mn_2(CO)_{10}$ matrix as $^{56}Mn(CO)_5$ which was subsequently detected radiochemically as $I^{56}Mn(CO)_5$.

More recently still, Wojcicki and Hallock[16] have shown that the 350-nm photolysis of $Mn_2(CO)_{10}$ in THF (corresponding to the σ-σ^* transition of the Mn-Mn bond[17]) produces an orange, paramagnetic complex which on standing at ambient temperatures slowly reverts to $Mn_2(CO)_{10}$. Addition of the orange solution to I_2 in THF under nitrogen gave 30–35% $Mn(CO)_5I$[16] whereas a solution of $Mn_2(CO)_{10}$ in THF does not react with I_2 under ambient

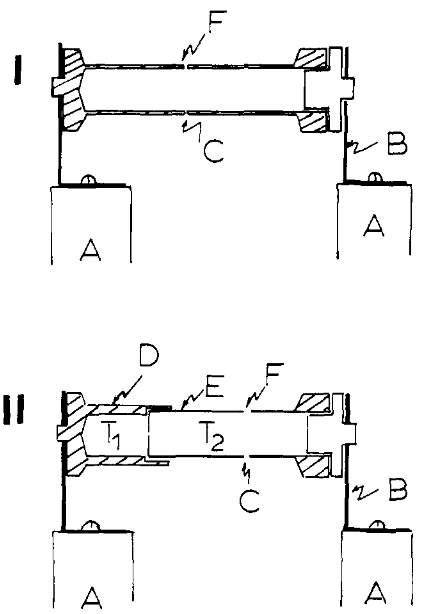

Figure 1. Design of (i) a single oven and (ii) a double oven tantalum Knudsen cell used for simultaneous matrix deposition and monitoring of metals (A = water-cooled copper electrodes, B = tantalum support clips and screws, C = orifice directed at quartz crystal microbalance, F = orifice directed at matrix, D = thick wall, E = thin wall (where temperature $T_2 > T_1$).

conditions.[16] The esr spectrum of the orange solution showed a six-line signal (^{55}Mn ($I = 5/2$)). Wojcicki and Hallock's results strongly suggest that the primary photolysis product of $Mn_2(CO)_{10}$ in suitable solvents is the radical $Mn(CO)_5$ which is a reasonably stable species with respect to $Mn_2(CO)_{10}$ or $Mn(CO)_n$ (where $n < 5$). Their results, however, do not eliminate the possibility of $Mn(CO)_5S$, a solvent stabilized intermediate. These results can be contrasted with those of Rest and Crichton[18] which show that the matrix photolysis of $Mn_2(CO)_{10}$ in Ar at 10°K produces $Mn_2(CO)_n$ (where $n < 10$; see later).

All of these studies clearly favor the existence of a $Mn(CO)_5$ radical. However, fundamental questions that remain to be answered relate to the molecular structure, geometry, bonding, and vibrational properties of $Mn(CO)_5$, a knowledge of which is basic to any discussion of its chemical reactions. Direct observation of the radical using matrix isolation infrared spectroscopy can in principle provide this information. In this section we report such data.

Experimental Section

Manganese (in powder form; A. D. Mackay, New York, N.Y., 99.99%, 325 mesh) was vaporized from a directly heated tantalum Knudsen cell. The wall thickness for single oven Knudsen cells was generally 0.015 in. with orifice sizes 0.1-1.0 mm. The furnace used for the evaporation of the metals has been described previously.[19] The rate of manganese deposition was continuously monitored by using a quartz crystal microbalance[20] set behind the Knudsen cell (the design of which is shown in Figure 1(i)) so as to receive the backward manganese flux effusing from a second orifice (labeled C in Figure 1(i)). For experiments in which superheating of the manganese vapor was required (see below) the double oven Knudsen cell shown in Figure 1(ii) was employed. In this design, the required temperature gradient is simply achieved by constructing the two chambers with walls of different thicknesses, thereby avoiding the necessity of having to heat the two chambers separately.[21] Temperature profile curves have been compiled for this double oven Knudsen cell for different lengths and wall thicknesses[22] and checked using an optical pyrometer. Temperature gradients of 500° between the two chambers were easily achieved.

Dimanganese decacarbonyl was purified by vacuum sublimation directly into a storage bulb, which was attached to the inlet system of a gas flow Knudsen cell for matrix deposition or pyrolysis experiments.

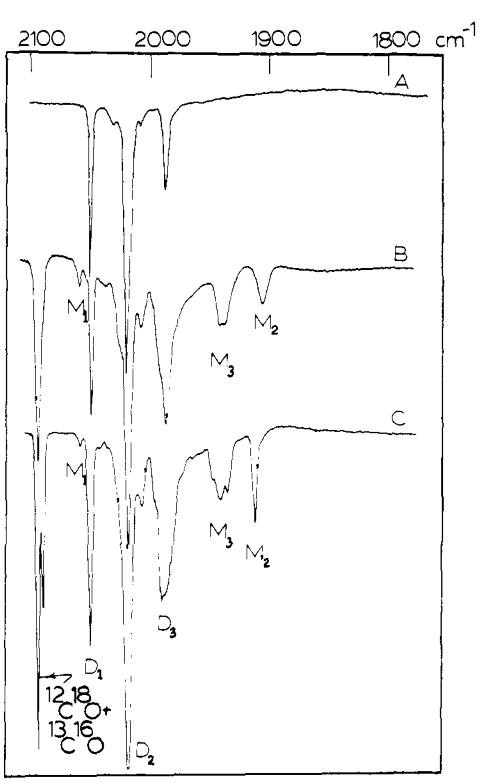

Figure 2. The matrix infrared spectra of (A) $Mn_2(CO)_{10}$ in Ar, (B) the products of the cocondensation reaction of manganese with $^{12}C^{16}O$:Ar = 1:5 (where the CO absorptions marked $M_{1,2,3}$ = $Mn(CO)_5$ and $D_{1,2,3}$ = $Mn_2(CO)_{10}$), and (C) the products of the cocondensation reaction of manganese with pure $^{12}C^{16}O$.

Research grade $^{12}C^{16}O$ (99.99%) and Ar (99.99%) were supplied by Matheson of Canada and $^{12}C^{18}O$ (50-55%) by Analytical Supplies (N.J.). Gas mixtures were prepared by conventional vacuum line techniques. Matrix gas flows, controlled by a calibrated micrometer needle valve, were usually in the range 2-8 mmol/hr. In the infrared experiments matrices were deposited on a CsI window cooled to either 15°K by means of an Air Products Displex closed cycle helium refrigerator or 10°K by an Air Products liquid helium transfer system. Spectra were recorded on a Perkin-Elmer 180 or 621 infrared spectrophotometer.

Results and Discussion

When manganese vapor effusing from a tantalum Knudsen cell was condensed with pure $^{12}C^{16}O$ onto a CsI plate cooled to 10-15°K (using Mn deposition rates arranged so that the probability of a Mn atom having another Mn atom as nearest neighbor in the fcc lattice of CO was approximately 1 in 10^3), the matrix infrared spectrum was essentially identical with that obtained from $Mn_2(CO)_{10}$ deposited in an argon matrix (Figure 2A). These results were somewhat disquieting in that the mass spectroscopic data[23] for manganese vapor effusing from a Knudsen cell under similar conditions to those used in our experiments establishes a vapor composition of about 99% atomic manganese. In addition Schnepp[24] and Mann[24] have studied the electronic spectrum of manganese vapor deposited into pure Ar at 4.2°K and obtained data consistent with the presence of matrix isolated Mn atoms with very little evidence for molecular Mn_n species. Even if molecular species such as Mn_2 had been formed along with atomic Mn, the chances of detecting them would be slight, as the molecular spectra would be dominated by the intense atomic spectrum of Mn (see for example ref 25a). Furthermore, at the high Mn-CO dilutions employed, one predicts statistically almost exclusive formation of mononuclear carbonyl species

$Mn(CO)_n$. However, our data show the exclusive production of the binuclear dimanganese decacarbonyl, $Mn_2(CO)_{10}$.

The three possible sources of $Mn_2(CO)_{10}$ were considered to be (i) diffusion and dimerization of a $Mn(CO)_5$ species in the matrix, (ii) high concentrations of Mn_2 effusing from the Knudsen cell, and (iii) surface diffusion and dimerization of Mn atoms during deposition. To establish the origin of the dimer the following experimental results were taken into consideration.

In the light of Rest and Crichton's[18] recent matrix photolysis experiments for $Mn_2(CO)_{10}$ in Ar, the diffusion of $Mn(CO)_5$ in Ar seems an unlikely source of $Mn_2(CO)_{10}$. Their results indicate that mononuclear carbonyl species are *not* formed on mercury arc photolysis of polynuclear carbonyl complexes in argon matrices, but instead $Mn_2(CO)_n$ species are favored. Although the $Mn_2(CO)_n$ products could not be characterized, the data strongly suggested that either the Mn–Mn bond is retained or that the bond is broken during photolysis but the $Mn(CO)_n$ fragments are too bulky to diffuse in argon and remain as nearest neighbors within the argon cage. On terminating the photolysis, the dimer species will re-form. Wojciki's result[16] and our warm-up data to be described later are consistent with this proposal.

In a number of different experiments in which the orifice size of the Knudsen cell was varied between 0.1 and 1.0 mm, the results with pure $^{12}C^{16}O$ were essentially the same. Thus, the possibility that Mn_2 dimers were being formed in supersonic molecular beams (see, for example, ref 25b) of manganese, effusing from the Knudsen cell with very small orifice diameters (0.1 mm), was considered to be most unlikely, as the results were essentially the same as those with large diameter orifices (1.0 mm).

Double oven Knudsen cell techniques were used to superheat the vapors effusing from the Knudsen cell. In these experiments, designed to dissociate any dimanganese to monatomic manganese, the results were found to be essentially the same as those of the single Knudsen cell experiments, showing only the formation of $Mn_2(CO)_{10}$, indicating the unlikelihood of Mn_2 being a major constituent of the effusing vapor.

However, when the Mn:CO ratio was reduced to 1:10^4 or less, it was found that in addition to the main $Mn_2(CO)_{10}$ carbonyl absorptions *three* new carbonyl absorptions grew in at 1938 ms (M_3), 1911 w (M_2), and *ca.* 2060 vw (M_1) cm^{-1} (Figure 2C and Table I).

Essentially the same results were obtained in concentrated CO:Ar = 1:5 matrices except that the line at about 1938 cm^{-1} showed less splitting[49] (Figure 2B and Table I) than that observed in pure CO. A series of careful experiments was performed to establish whether M_1, M_2, and M_3 belonged to the same species. A number of runs were performed in which different rates of Mn deposition were used between runs and in the same run. Using absorbance measurements and taking into account the matrix splittings, the intensity ratio M_1:M_2:M_3 (in a particular matrix material) remained essentially constant (Table II), suggesting that they be assigned to a single species. Although this new species was reluctant to diffuse at temperatures as high as 40–45°K (where argon is slowly boiling off), a slow decrease in the intensities of the three new bands M_1, M_2, and M_3 was observable. However, the intensitv ratio M_1:M_2:M_3 during warm-up remained approximately constant, supporting the view that they are all associated with a single species.

Table I. Infrared Spectra of the Products of the Condensation Reaction of Manganese with Pure CO and Concentrated CO:Ar = 1:5 Matrices at 10°K

Matrix isolated $Mn_2(CO)_{10}$ in Ar at 10°K	Mn with pure $^{12}C^{16}O$	Mn–$^{12}C^{16}O$/Ar (1/5)	Assignment
	2059 w	2058 w	$Mn(CO)_5$
2050 s	2049 s	2048 s	$Mn_2(CO)_{10}$
2017 vs	2016 vs	2015 vs	$Mn_2(CO)_{10}$
2007 w	2005 w	2005 w	$Mn_2(CO)_{10}$
1986 s	1989 s	1985 s	$Mn_2(CO)_{10}$
	1945 mw 1939 ms 1933 m [a]	1940 ms 1936 ms	$Mn(CO)_5$
	1911 ms	1904 ms	$Mn(CO)_5$

[a] Matrix splitting owing to the low substitutional site symmetry in the crystal lattice of solid CO.

Table II. Infrared Spectra for $V(CO)_5$, $Cr(CO)_5$, $Mn(CO)_5$, and $Cr(CO)_5^-$ in the CO Stretching Region

$V(CO)_5$ (ref 26)	$Cr(CO)_5$[a] (ref 28)	$Mn(CO)_5$[b] (in Ar)	$Cr(CO)_5^-$ (ref 29)
	2093 vvw	2060 (0.141)	Not obsd
1947 s[c]	1965 s	1938 (1.000)[c]	1855 s[c]
1920 m	1936 ms	1911 (0.378)	1838 m

[a] The data used are for the square pyramidal fragment $Cr(CO)_5$ in argon matrices.[28] [b] Relative absorption intensities for $Mn(CO)_5$ are shown in parentheses and are normalized to unity for the most intense line. The absorbances were obtained by the method described in ref 1. [c] These lines show a small doublet splitting in argon matrices (see text).

These results for manganese are analogous in many respects to our data for the Co–CO reaction[2,26] which yields cobalt tetracarbonyl, $Co(CO)_4$, under conditions of slow Co deposition, yet exclusively $Co_2(CO)_8$ with high Co deposition rates. By analogy with the cobalt data and for the reasons to be described, we assign the new species in the Mn–CO system to manganese pentacarbonyl, $Mn(CO)_5$.[50] It would therefore appear that the relative concentration of dinuclear to mononuclear species depends on the manganese atom concentration, the mononuclear species being favored at very low Mn concentrations (see Figure 2B and C), indicating that Mn_2 probably forms in a surface diffusion reaction, presumably in the "quasi-liquid phase" existing in the transition from the vapor to the solid during matrix condensation.

The assignment of $Mn(CO)_5$ shown in Table II is based on the number, frequencies, and relative intensities of the observed carbonyl stretching modes. For a C_{4v} square pyramidal pentacarbonyl, theory predicts three infrared-active

$$\Gamma_{\text{vib}}^{\nu\text{CO}} = \underset{(\text{IR/R})}{2A_1} + \underset{(\text{IR/R})}{E} + \underset{(\text{R})}{B_1}$$

modes, which can best be described as A_1 apical and A_1 and E equatorial CO stretching modes. For an angle C_{ap}–Mn–C_{eq} close to 90°, the equatorial A_1 mode should appear as a *weak*, high frequency line while the equatorial E and apical A_1 modes should appear at considerably lower frequencies with the E mode being of higher frequency and more intense (approximately 4:1). On the other hand, for a D_{3h} trigonal bipyramidal pentacarbonyl *two* infrared-active

$$\Gamma_{\text{vib}}^{\nu\text{CO}} = \underset{(\text{R})}{2A_1'} + \underset{(\text{IR})}{A_2''} + \underset{(\text{IR/R})}{E'}$$

modes are predicted, an A_2'' axial and an E' equatorial CO stretching mode, both of which are expected at lower frequencies than their respective (Raman active) A_1' modes. The A_2'' mode should be at *higher* frequencies than the E' mode with an intensity ratio of 2:3.

Table III. Cotton–Kraihanzel Bond Stretching Force Constants[a] for $Mn(CO)_5$ and Related $XMn(CO)_5$ Complexes (where X = H, Cl, Br, I, and $Mn(CO)_5$)

Complex	$k_{CO}{}^{ap}$	$k_{CO}{}^{eq}$	$k_i{}^b$	Ref
$Mn(CO)_5$	14.76	15.76	0.30	This study
$(CO)_5MnMn(CO)_5$	15.91	16.52	0.08	33
$HMn(CO)_5$	16.42	16.93	0.26	46
$ClMn(CO)_5$	16.24	17.51	0.22	30
$BrMn(CO)_5$	16.35	17.41	0.25	30
$IMn(CO)_5$	16.38	17.29	0.23	30

[a] In mdyn/Å. [b] In these calculations k_i is the cis K_{COCO} interaction force constant where it was assumed that $2k_i{}^{cis} = k_i{}^{trans}$.

Our observations of *three* lines at 2060, 1938, and 1911 cm^{-1} with the relative intensities shown in Table II are consistent with the C_{4v} square pyramidal assignment. The assignment is further strengthened by comparison of the infrared data with that for $V(CO)_5$,[26] $Cr(CO)_5$,[28] $Cr(CO)_5^-$ [29] (Table II), and indeed any $Mn(CO)_5X$ species (X = H, Cl, Br, I, Me) containing the C_{4v} $Mn(CO)_5$ residue.[30] As expected, the CO stretching frequencies for $Mn(CO)_5$ lie *above* those of the isoelectronic species $Cr(CO)_5^-$. The computed Cotton-Kraihanzel[31] CO bond stretching force constants for $Mn(CO)_5$ are shown in Table III and like pentacarbonyl Mn(I) derivatives[30,32] exhibit $k_{CO}{}^{eq} > k_{CO}{}^{ap}$. Unfortunately these values cannot be compared with $Cr(CO)_5^-$ as the high frequency A_1 CO stretching mode was not reported.[29] It is also interesting that the $k_{CO}{}^{eq}$ and $k_{CO}{}^{ap}$ values for $Mn(CO)_5$ are less than the respective force constants for the dimer $Mn_2(CO)_{10}$[33] (Table III and see next section).

Intensity Calculations and the Molecular Geometry of $Mn(CO)_5$. The intensity ratio $I_2{:}I_1$ for the A_1 equatorial and apical CO stretching modes of complexes containing a square pyramidal $M(CO)_5$ group has been of considerable interest[34] primarily because it is directly related to the C_{eq}–M–C_{ap} bond angle θ through the analytical expression[35a]

$$\frac{I_2}{I_1} = \left[\frac{\rho\mu_a + 2\mu_e\cos\theta}{\mu_a - 2\rho\mu_e\cos\theta}\right]^2 \qquad \text{(I)}$$

Within the restrictions of the Cotton-Kraihanzel force field, the derivation of eq I is quite rigorous, in that vibrational coupling between the symmetry coordinates has been included and different transition dipole moments for apical (μ_a) and equatorial (μ_e) CO groups have been taken into account. The quantity ρ is related to the Cotton-Kraihanzel force constants.[35a] An additional expression can be derived for square pyramidal $M(CO)_5$ which involves the intensities of the A_1 equatorial and apical and the E equatorial CO stretching modes as shown in eq II. Thus by combining eq I

$$\frac{I_1 + I_2}{I_3} = \frac{\mu_a^2 + 4\mu_e^2\cos^2\theta}{4\mu_e^2\sin^2\theta} \qquad \text{(II)}$$

and II it is possible to solve for both the angle θ and the ratio of the transition dipole moments for axial and equatorial CO groups. Expression I has been used to evaluate the angle θ for a number of $XMn(CO)_5$ complexes where the observed order, H > Cl > Br > I, was explained in terms of increased repulsions between the Mn-X and equatorial Mn-CO bonding electrons.[35a] $Mn(CO)_5$ is therefore of central interest in these discussions, as it may be regarded as the "parent" complex of the series, X now being a *geometrically* vacant coordination site. Whether or not the odd valence electron of $Mn(CO)_5$ is localized in this site or delocalized into the π system is a question of some importance.

It has been shown previously[35a] that if mixing of the A_1 axial and equatorial CO stretching modes is the only means by which the equatorial mode can gain intensity, then ρ^2 equals I_2/I_1. However, for $Mn(CO)_5$, $\rho^2 = 0.065$, yet $I_2/I_1 = 0.371$ and it is clear that some other effect in addition to coupling must be responsible for the intensity of the equatorial mode (*cf.* $Mo(CO)_5L$[35b] and $Mn(CO)_5X$).[35a] This difference in intensity ratio might be attributed to either a deviation from planarity for the four equatorial CO groups or to a difference in the transition dipole moments for the axial and equatorial CO groups in the A_1 symmetry modes.

Using the Cotton-Kraihanzel force constants and infrared absorbances (measured in Ar matrices) listed in Tables II and III, and assuming initially that $\mu_a \simeq \mu_e$, expression I can be used to solve for the angle θ. With this approximation we arrive at 81.2° for the angle θ (which gives 88.5° for the equatorial OC-Mn-CO angle). For an uncertainty of 5% in our absorbance measurements, an uncertainty of ±2.2° is introduced in the angle θ.

Alternatively, if we use expressions I and II and solve for θ and μ_a/μ_e, we arrive at 80.5° and 1.07, respectively. Clearly both approaches yield values for θ close to 81° which can be compared with the calculated value 96.5° for $HMn(CO)_5$[35c] and the X-ray diffraction value 97° for $HMn(CO)_5$ and $Mn_2(CO)_{10}$.[36,37] We therefore conclude that the angle θ takes the order $HMn(CO)_5 > ClMn(CO)_5 > BrMn(CO)_5 > IMn(CO)_5 > Mn(CO)_5$.

One possible rationale for the observed trend in the angle θ is the following. To begin with, manganese in $Mn(CO)_5$ is formally Mn(0) whereas manganese in $XMn(CO)_5$ is Mn(I). Therefore the observed increase in Mn-CO π-bonding in $Mn(CO)_5$ compared to $XMn(CO)_5$ or $Mn_2(CO)_{10}$, as indicated by their respective Cotton-Kraihanzel bond stretching force constants (Table III), is understandable. However, if one accepts the electron repulsion and steric arguments alluded to earlier, to explain the order H > Cl > Br > I for $XMn(CO)_5$, then one is forced to conclude that the smaller value of θ for $Mn(CO)_5$ is indicative of an electron repulsion effect between the equatorial Mn-C bonding electrons and the electron(s) in the vacant site which more than counterbalances the effect of the repulsions between the axial and equatorial Mn-C bonding electrons. However, without definitive evidence as to the electronic structure of $Mn(CO)_5$, discussions of this type can only be regarded as speculative.

The Structure and Bonding of Transition Metal Pentacarbonyls and Pentacarbonyl Anions. Using matrix synthetic techniques, a number of new pentacarbonyl species have become accessible to study by spectroscopic methods of analysis. The infrared spectra of these species have been most informative, establishing the molecular structures shown in Table IV. Isoelectronic species are grouped together according to whether they contain 15, 16, 17, or 18 electrons in their outer valence shells, and it can be seen that isoelectronic species (presumably in their most stable configurations) are also isostructural. These stereochemical changes are clearly electronic in origin and can be rationalized most

Table IV. Molecular Structures and Electronic Configurations of Some Pentacarbonyl Species

Pentacarbonyl	Stereochemistry[a]	No. of valence shell electrons	Ref
$V(CO)_5$	S.P.	15	26
$Cr(CO)_5$	S.P.	16	28
$Mn(CO)_5$	S.P.	17	This study
$Cr(CO)_5^-$	S.P.	17	29
$Fe(CO)_5$	T.B.	18	47
$Mn(CO)_5^-$	T.B.	18	48

[a] S.P. = Square pyramidal, T.P. = Trigonal bipyramidal.

easily in terms of the generally accepted MO sequences for transition metal trigonal bipyramidal and square pyramidal complexes,[38a] ... $(3a_1')(3e')(3a_2'')[(3e'')(4e')(4a_1')](5e')$ ... and ... $(a_2)(e)[(e)(b_2)(b_1)(a_1)](a_1)$ ... respectively, where the d orbital manifolds are enclosed in brackets.

Assuming that the low spin configuration is adopted by the $M(CO)_5$ species, which is not unreasonable in the light of, for example, low spin $Cr(CO)_6$, then it is seen that the $e''(d_{yz}, d_{xz})$ levels are filled and the $e'(d_{x^2-y^2}, d_{xy})$ levels partially filled for the 15- and 17-electron pentacarbonyls. These molecules will both be subject to first-order Jahn–Teller[39] distortions from a D_{3h} trigonal bipyramidal toward a C_{4v} square pyramidal structure. The latter itself is not unstable with respect to first-order Jahn–Teller distortions[51] but the 17-electron system is predicted to be unstable with respect to a B_1 vibration toward a C_{2v} structure through a second-order Jahn–Teller (SOJT) effect.[38a] Whether this instability is of a kinetic type (*i.e.*, a finite but low activation barrier) leading to facile interconversion of C_{2v} and C_{4v} forms, or whether it is thermodynamic so that there is effectively no barrier to the $C_{4v} \rightarrow C_{2v}$ distortion, the latter form being more stable, appears to depend on the energy gap between the highest filled and lowest empty molecular orbital.[38a]

The 16- and 18-electron, low spin pentacarbonyls are stable toward first-order Jahn–Teller distortions in either the D_{3h} or C_{4v} forms. The 16-electron system exemplified by $Cr(CO)_5$ is, however, predicted to be SOJT stable only in the low spin square pyramidal form. Low spin, trigonal bipyramidal $Cr(CO)_5$ is SOJT unstable with respect to the e′ vibration and will move toward the square pyramidal structure. In this context we would like to revise our previous discussion of the $Cr(CO)_5$ species.[27] As is now well known, $Cr(CO)_5$ can be synthesized from both Cr atom CO–Ar matrix cocondensations[27] and $Cr(CO)_6$–Ar matrix photolysis reactions.[28] However, $^{12}C^{16}O$–$^{13}C^{16}O$–Ar mixed isotope experiments have shown that the Cr atom technique yields trigonal bipyramidal $Cr(CO)_5$[27] whereas the photochemical route[28] leads to the square pyramidal form. Particularly interesting are the warm-up experiments which we have recently performed on the trigonal bipyramidal form of $Cr(CO)_5$ which at 40–45°K shows a reversal in the absorption intensities of the two observed CO stretching modes at 1964 and 1937 cm^{-1} from the original 2:3 ratio, observed on deposition, toward the 4:1 situation described for square pyramidal $Cr(CO)_5$.[28] The results authenticate the existence of a trigonal bipyramidal form of $Cr(CO)_5$ at 10–15°K which, on thermal annealing at 40–45°K, undergoes a kinetically slow skeletal rearrangement to the square pyramidal form of $Cr(CO)_5$ implying that of the "truly pentacoordinate species" the square pyramidal form is the thermodynamically most stable. These observations are related to Pearson's[38a] predictions of SOJT stability for C_{4v} $Cr(CO)_5$ but instability for D_{3h} $Cr(CO)_5$ toward the square pyramidal structure although it should be noted that the chromium atom in square pyramidal $Cr(CO)_5$[28] is in fact weakly solvated in its vacant coordination site by the atoms or molecules constituting the matrix (*e.g.*, Ne, Ar, Kr, Xe, CO, CH_4, CF_4, or SF_6).[53]

The 18-electron pentacarbonyls on the other hand are predicted to show SOJT instability in both the D_{3h} and C_{4v} configurations, providing the energy gap is small enough. This instability is evidently not sufficient to make the intermediate C_{2v} form the most stable, but interconversion of apical and equatorial carbonyl ligands is evidently very easy, as seen by the room temperature ^{13}C nmr equivalence of axial and equatorial CO groups in $Fe(CO)_5$, presumably operating *via* the $D_{3h} \leftrightarrow C_{4v}$ mechanism.

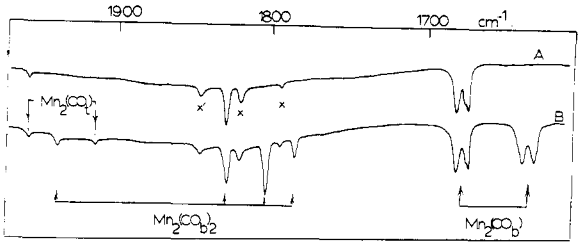

Figure 3. The matrix infrared spectrum of the products of the cocondensation reaction of manganese vapor with (A) $^{12}C^{16}O$:Ar $\simeq$ 1:250 and $^{12}C^{16}O$:$^{12}C^{18}O$:Ar $\simeq$ 1:1:500 at 10°K (where X′ refers to $Mn^{12}C^{16}O$ and X refers to impurity lines; see text).

Dimanganese Monocarbonyl, $Mn_2(CO_b)$, and Dimanganese Dicarbonyl, $Mn_2(CO_b)_2$. Matrix cocondensation reactions were performed involving manganese atoms and *dilute* CO–Ar matrices, using Mn deposition rates which favor the formation of Mn_2. The matrix infrared spectrum using $^{12}C^{16}O$:Ar $\simeq$ 1:250 is shown in Figure 3. *Two* prominent CO absorptions are observed at 1835.4 cm^{-1} and 1688–1680 cm^{-1} (where the closely spaced doublet at 1688–1680 cm^{-1} is a matrix site splitting) and $Mn_2(CO)_{10}$ is noticeably *absent*.[52] Using an isotopic mixture $^{12}C^{16}O$:$^{12}C^{18}O$:Ar $\simeq$ 1:1:500, the matrix infrared spectrum shown in Figure 3B was obtained in which a characteristic isotope pattern[38b] of a symmetrical dicarbonyl and a monocarbonyl are easily discernible (see Table V for the vibrational assignments).

Table V. Isotopic Frequencies and Vibrational Assignments for the Binuclear Manganese Carbonyls $Mn_2(CO)_n$ (where n = 1 or 2)

Obsd Frequency (cm^{-1})	Calcd Frequency[c] (cm^{-1})	Vibrational assignment[a]
1964.4		$Mn_2(^{12}C^{16}O_t)$
1920.6		$Mn_2(^{12}C^{18}O_t)$
1945.6	1945.6	$Mn_2(^{12}C^{16}O_b)(^{12}C^{18}O_b)$
1835.4	1835.3	$Mn_2(^{12}C^{16}O_b)_2$
1809.6	1809.2	$Mn_2(^{12}C^{16}O_b)(^{12}C^{18}O_b)$
1790.6	1791.1	$Mn_2(^{12}C^{18}O_b)_2$
1688.2–1680.0[b]		$Mn_2(^{12}C^{16}O_b)$
1646.4–1638.2[b]		$Mn_2(^{12}C^{18}O_b)$

[a] Key: t = terminal and b = bridging CO groups. [b] Matrix splitting. [c] The CO stretching force constants for $Mn_2(CO_b)_2$ which gave the best fit for the frequencies were f_r = 14.61 and f_{rr} = 1.00 mdyn/Å. The CO stretching force constants calculated for $Mn_2(CO_t)$ and $Mn_2(CO_b)$ are 15.58 and 11.45 mdyn/Å, respectively.

Matrix warm-up experiments at about 25–30°K showed the dicarbonyl to grow at the expense of the monocarbonyl.

Frequency calculations were performed on the mixed isotopic dicarbonyls $Mn_2(^{12}C^{16}O)_n(^{12}C^{18}O)_{2-n}$ (where n = 0–2) assuming the Cotton–Kraihanzel force field approximation.[31] A least-squares analysis of the data was performed by adjusting the values of the two parameters f_r and f_{rr} to yield the set of frequencies shown in Table V. The agreement between the observed and calculated frequencies is excellent for all CO stretching modes and provides convincing evidence that our assignment of $Mn_2(CO_b)_2$ is correct.

On the basis of the very low frequencies of these carbonyl stretching modes when compared to $Mn_2(CO)_{10}$, together with the prior knowledge that Mn_2 should constitute a major proportion of the reacting metal species in the matrix under the experimental conditions used, we propose that the data are best interpreted in terms of a binuclear bridged monocarbonyl species $Mn_2(CO_b)$ (I) and a binuclear dicarbonyl bridged species $Mn_2(CO_b)_2$ (II) as shown below. Although we have assumed the existence of a Mn–Mn bond in species I and II, matrix esr measurements would be required to establish whether this is the case in practice. Charge delocalization of Mn_2 electrons into the π^* orbitals of the ketonic CO groups is possible for both molecules, but to a lesser extent in $Mn_2(CO_b)_2$ compared to $Mn_2(CO_b)$, as the latter is formally Mn(I) whereas the former is Mn(II). Thus a rise to higher CO stretching frequencies on passing from $Mn_2(CO_b)$ to $Mn_2(CO_b)_2$ is understandable.

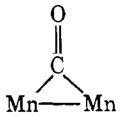

I

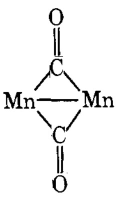

II

Dimanganese Monocarbonyl, $Mn_2(CO_t)$. In these dilute CO–Ar experiments a high frequency CO stretching mode at 1964.4 cm^{-1} accompanied those assigned to $Mn_2(CO_b)$ and $Mn_2(CO_b)_2$. In the mixed isotope $^{12}C^{16}O$:$^{12}C^{18}O$:Ar $\simeq$ 1:1:500 experiment a *single* counterpart to the 1964.4 cm^{-1} absorption was observed at 1920.6 cm^{-1} which has approximately the correct isotope shift for the monocarbonyl (Figure 3). As this species absorbs at considerably higher frequencies than those assigned to the binuclear bridged carbonyls, $Mn_2(CO_b)_n$, as well as to the binary mononuclear carbonyls, $Mn(CO)_m$ (see next section), we accordingly assign it to the binuclear terminal monocarbonyl, $Mn_2(CO_t)$.

Manganese–Carbon Monoxide Cocondensation Reactions at Intermediate CO:Ar Ratios. When matrix experiments were performed under conditions of intermediate dilution ($^{12}C^{16}O$:Ar $\simeq$ 1:50–1:100) the spectra so obtained were complex (Table VI) showing a large number of carbonyl stretching modes in the region (2090–1676 cm^{-1}) and are difficult to interpret with any degree of certainty. A few generalizations, however, can be drawn from the spectra. For example, a number of absorptions appear in the region 1940–1850 cm^{-1} which by comparison with the $Mn(CO)_5$ data indicates the presence of binary *mononuclear* carbonyls, $Mn(CO)_m$ (where m = 1–5).

Tentative assignments for these mononuclear binary carbonyls can be made on the basis of their concentration and warm-up characteristics, the most likely assignments being those shown in Table VI.

In addition to the $Mn(CO)_n$ absorptions, *two* other main groups of lines are observed. One group appears at *lower* frequencies, in the range 1840–1676 cm^{-1}, and is assigned to bridged binuclear carbonyls, $Mn_2(CO_b)_n$, as described earlier. The second group appears at *higher* frequencies in the range 2068–1958 cm^{-1} and suggests the presence of binuclear carbonyls, $Mn_2(CO_t)_n$, containing terminal CO groups. Warm-up of these matrices to 40°K causes all of the mononuclear and bridged binuclear carbonyl lines in the 1940–1676-cm^{-1} region to decrease in intensity and eventually to disappear, with the concomitant growth of lines in the $Mn_2(CO_t)_n$ 2068–1958-cm^{-1} region. The final spectrum showed the presence of $Mn_2(CO)_{10}$ as the major product although some medium intensity lines remained (Table VI) suggesting the presence of $Mn_2(CO)_l$ (where l has values probably close to ten).

Apart from $Mn_2(CO)_{10}$, $Mn(CO)_5$, $Mn_2(CO_t)$, $Mn_2(CO_b)_2$, and $Mn_2(CO_b)$, it was impossible to collect definitive isotope data for the remaining carbonyls, owing mainly to the large number of different species present in the matrix at any one time and the inevitable complication of band overlap of isotopic multiplets.

Table VI. Matrix Infrared Spectra of the Products of the Manganese–Carbon Monoxide Reaction at Intermediate CO:Ar = 1:50–1:100 Ratios[a]

Frequency (cm^{-1})	Specific assignment	General assignment
2068		$Mn_2(CO)_t)_l$
2056[c]		
2048[c]	$Mn_2(CO)_{10}$	
2036[c]		
2038		
2018[c]	$Mn_2(CO)_{10}$	
2004		
1990		
1984[c]	$Mn_2(CO)_{10}$	
1968		
1965[c]		
1958[b,f,g]	$Mn_2(CO_t)$	
1940[d]	$Mn(CO)_5$	$Mn(CO)_m$
1933[d]		
1926	$Mn(CO)_4$	
1919		
1910[d]	$Mn(CO)_5$	
1890	$Mn(CO)_3$	
1858	$Mn(CO)_2$	
1850	$Mn(CO)$	
1866[e]	$Mn_2(CO_b)_3$	$Mn_2(CO_b)_n$
1832[b,f,g]	$Mn_2(CO_b)_2$	
1683[b,f,g]	$Mn_2(CO_b)$	

[a] Only frequencies have been listed; intensity changes during warm-up experiments and vibrational assignments (general and specific) are discussed in the text. [b] Strongest lines on 10°K deposition at CO:Ar $\cong$ 1:50. [c] Lines remaining after warm-up to 40–45°K. [d] Assigned to $Mn(CO)_5$ from the pure CO and concentrated CO–Ar experiments (see text). [e] Warm-up behavior favors a binuclear assignment to this species. [f] Species characterized by mixed $^{12}C^{16}O$–$^{12}C^{18}O$ isotope substitution studies. [g] Strongest lines on 10°K deposition at CO:Ar = 1:250.

The Relationship between $Mn_2(CO)_n$ (where n = 1 or 2) and CO Chemisorbed on Mn. The infrared spectrum of CO chemisorbed on polycrystalline metal films usually contains two broad bands, a high frequency and a low frequency CO stretching mode.[40] Moskovits and Ozin have recently suggested that a connection exists between our earlier studies of matrix isolated monocarbonyl species, MCO (where M = V, Fe, Co, Ni, Cu, Pd, and Pt), and CO chemisorbed on the corresponding metal films.[41] In all cases it was found that the lower frequency CO stretching mode of chemisorbed CO has a *lower* frequency than the CO mode of the corresponding triatomic molecule. These results corroborate the suggestion of Eischens[42] and Mason's[43] single-crystal LEED evidence for CO on Pt, that the lower frequency line of chemisorbed CO corresponds to a *bridge*-bonded carbonyl and the higher frequency line to a terminally bonded carbonyl, rather than Blyholder's[44] suggestion of terminal CO groups on corner and edge surface sites, respectively.

When relating our matrix MCO data to the corresponding CO chemisorption data on M, discussions have always been restricted to mononuclear species. However, the manganese-carbon monoxide system of this study presents a unique opportunity to examine the "terminal and bridge" chemisorption process with respect to the terminal and bridged binuclear species $Mn_2(CO_t)_n$ and $Mn_2(CO_b)_n$. The 1950-cm^{-1} absorption corresponding to terminal CO chemisorbed on manganese lies as expected at higher frequencies than the 1850-cm^{-1} absorption assigned to MnCO. However, the 1964-cm^{-1} absorption assigned to terminally bonded CO in $Mn_2(CO_t)$ is almost *coincident* with that for terminally chemisorbed CO on Mn. It is therefore apparent that the charge available for back-donation from the appropriate Mn_2 π-type orbitals to the π^* orbitals of CO in $Mn_2(CO_t)$ is comparable to the charge delocalization from the surface Mn atoms to one type of chemisorbed CO. Although this agreement between the CO stretching absorptions may be purely coincidental, it could actually be reflecting a genuine "localized bonding interaction" for terminally chemisorbed CO on Mn, a view held by some who have dwelt on the existence of localized states in quantum mechanical calculations for chemisorption on idealized semi-infinite model crystals.[45] To what extent localized orbitals are formed by real systems is as yet an unanswered question, although it would appear to depend on the atomic orbital energy levels of adsorbate to adsorbent and whether the absorbent is terminally or bridge bonded.

Additional information for the chemisorption process can be derived from $Mn_2(CO_b)$ which adsorbs at a considerably lower frequency ($\sim$1684 cm^{-1}) than the bridge mode of CO chemisorbed on Mn (1890 cm^{-1}). The introduction of a second bridging CO ligand to give $Mn_2(CO_b)_2$ results in a *substantial* shift to 1835 cm^{-1}, only 55 cm^{-1} lower than the bridge form of chemisorbed CO on Mn.

These results could imply that the association of a bridging CO group with a manganese surface is not as localized an interaction as that of a terminal CO group and may suggest that at least two CO ligands bridge, but only one CO ligand terminally bonds, to a surface manganese atom.

Discussions of this kind are of course highly speculative and open to criticism, but it is probably fair to say that results of this type can in principle give a great deal of chemical insight into the nature of the bonding of CO to surface metal atoms and would reinforce the view that the interactions between molecules and surfaces upon chemisorption are in many ways similar to those operating in normal metal-ligand coordination complexes.

Acknowledgments. We would like to thank Dr. Martin Moskovits for many stimulating and helpful discussions. We also gratefully acknowledge the skillful technical assistance of Mr. B. Torbet and Mr. A. Campbell and the financial assistance of the Research Corporation and the National Research Council of Canada.

References and Notes

(1) H. Huber, E. P. Kündig, M. Moskovits, and G. A. Ozin, *J. Amer. Chem. Soc.*, **95**, 332 (1973).

(2) G. A. Ozin in "The Vibrational Spectra of Trapped Species," Ed. H. Hallam, Wiley, New York, N.Y., 1973.

(3) L. W. Yarbrough II, G. V. Calder, and J. G. Verkade, *J. Chem. Soc., Chem. Commun.*, 705 (1973); H. Huber, M. Moskovits, and G. A. Ozin, *Inorg. Chem.*, In press.

(4) E. P. Kündig, M. Moskovits, and G. A. Ozin, *Can. J. Chem.*, **51**, 2737 (1973).

(5) H. Huber, W. Klotzbücher, G. A. Ozin, and A. Vander Voet, *Can. J. Chem.*, **51**, 2722 (1973).

(6) E. P. Kündig, M. Moskovits, and G. A. Ozin, *Can. J. Chem.*, **51**, 2710 (1973); D. W. Green, J. Thomas, and D. M. Gruen, *J. Chem. Phys.*, **58**, 5453 (1973).

(7) W. Klotzbücher and G. A. Ozin, *J. Amer. Chem. Soc.*, **91**, 3790 (1973).

(8) A. Kant, S. S. Lin, and B. Strauss, *J. Chem. Phys.*, **49**, 1983 (1968).

(9) G. A. Ozin and A. Vander Voet, *Accounts of Chem. Res.*, **6**, 313 (1973).

(10) D. R. Bidlnosti and W. S. McIntyre, *Can. J. Chem.*, **48**, 593 (1970); *Chem. Commun.*, 555 (1966).

(11) J. P. Fawcett, A. J. Poë, and M. V. Twigg, *J. Organometal. Chem.*, **51**, C17 (1973).

(12) L. I. B. Haines and A. J. Poë, *Nature* (*London*), **215**, 699 (1967); **218**, 562 (1968).

(13) C. H. Bamford and C. A. Finch, *Trans. Faraday Soc.*, **59**, 540 (1963); C. H. Bamford and R. Denyer, *ibid.*, **62**, 1567 (1966).

(14) D. J. Hopgood, Ph.D. Thesis, London University, 1966.

(15) I. G. De Jong, S. C. Srinivasan, and D. R. Wiles, *Can. J. Chem.*, **47**, 1327, (1969); *J. Organometal. Chem.*, **26**, 119 (1971).

(16) S. A. Hallock and A. Wojcicki, *J. Organometal. Chem.*, **54**, C27 (1973).

(17) R. A. Levenson, H. B. Gray, and G. P. Ceasar, *J. Amer. Chem. Soc.*, **92**, 3653 (1970).

(18) A. J. Rest and O. Crichton, private communication.

(19) E. P. Kündig, M. Moskovits, and G. A. Ozin, *J. Mol. Struct.*, **14**, 137 (1972).

(20) M. Moskovits and G. A. Ozin, *Appl. Spectrosc.*, **26**, 481 (1972).

(21) J. M. Brom and W. Weltner, *J. Mol. Spectrosc.*, **45**, 82 (1973).

(22) M. Moskovits, unpublished work.

(23) A. Kant and B. Strauss, *J Chem Phys.*, **41**, 3806 (1964).

(24) O. Schnepp, *J. Phys. Chem. Solids*, **17**, 188 (1961); D. M. Mann and H. P. Broida, *J. Chem. Phys.*, **55**, 84 (1971).

(25) (a) S. Schoch and E. Kay, *J. Chem. Phys.*, **59**, 718 (1973); (b) S. E. Novick, T. B. Davies, T. R. Dyke, and W. Klemperer, *J. Amer. Chem. Soc.*, **95**, 8547 (1973), and references therein.

(26) E. P. Kündig, M. Moskovits, and G. A. Ozin, unpublished work.

(27) E. P. Kündig and G. A. Ozin, *J. Amer. Chem. Soc.*, **96**, 3820 (1974).

(28) M. A. Graham, M. Pollakoff, and J. J. Turner, *J. Chem. Soc. A*, 2939 (1971); M. A. Graham, R. N. Perutz, M. Poliakoff, and J. J. Turner, *J. Organometal. Chem.*, **34**, C34 (1972).

(29) P. A. Breeze and J. J. Turner, *J. Organometal. Chem.*, **44**, C7 (1972).

(30) H. G. Kaesz, R. Bau, D. Hendrickson, and J. M. Smith, *J. Amer. Chem. Soc.*, **89**, 2844 (1967), and references therein.

(31) F. A. Cotton and C. S. Kraihanzel, *J. Amer. Chem. Soc.*, **84**, 4432 (1962).

(32) M. B. Hall and R. F. Fenske, *Inorg. Chem.*, **11**, 1619 (1972).

(33) N. Flitcroft, D. K. Huggins, and H. D. Kaesz, *Inorg. Chem.*, **3**, 1123 (1964).

(34) L. M. Haines and M. H. B. Stiddard, *Advan. Inorg. Chem. Radiochem.*, in press.

(35) (a) A. R. Manning and J. R. Miller, *J. Chem. Soc. A*, 1521 (1966); (b) D. J. Darensbourg and T. L. Brown, *Inorg. Chem.*, **7**, 959 (1968); (c) P. S. Braterman, R. Bau, and H. G. Kaesz, *ibid.*, **6**, 2097 (1967).

(36) S. J. La Placa, W. C. Hamilton, and J. A. Ibers, *Inorg. Chem.*, **3**, 1491 (1964).

(37) R. E. Rundle and L. F. Dahl, *J. Chem. Phys.*, **26**, 1750 (1951).

(38) (a) R. G. Pearson, *J. Amer. Chem. Soc.*, **91**, 1252, 4947 (1969); (b) E. P. Kündig, D. McIntosh, M. Moskovits, and G. A. Ozin, *J. Amer. Chem. Soc.*, **95**, 7234 (1973); J. H. Darling and J. S. Ogden, *J. Chem. Soc., Dalton* Trans., 2496 (1972).

(39) H. A. Jahn and E. Teller, *Proc. Roy. Soc., Ser A*, **161**, 220 (1937).

(40) G. Blyholder and M. C. Allen, *J. Amer. Chem. Soc.*, **91**, 3158 (1969), and references therein.

(41) M. Moskovits and G. A. Ozin, *J. Chem. Phys.*, **58**, 1251 (1973); E. P. Kündig, D. McIntosh, M. Moskovits, and G. A. Ozin, *J. Amer. Chem. Soc.*, **95**, 7324 (1973); M. Moskovits and G. A. Ozin in "Vibrational Spectra and Structure," J. Durig, Ed., Marcel Dekker, New York, N.Y., 1974.

(42) R. P. Eischens, S. A. Francis, and W. A. Pliskin, *J. Phys. Chem.*, **60**, 194 (1956).

(43) R. Mason, private communication.

(44) G. Blyholder and M. C. Allen, *J. Phys. Chem.*, **68**, 2772 (1964).

(45) J. Koutecky, *Advan. Chem. Phys.*, **9**, 85 (1965); T. B. Grimley, *Advan. Catal. Relat. Subj.*, **12**, 1 (1960).

(46) D. K. Huggins and H. D. Kaesz, *J. Amer. Chem. Soc.*, **86**, 2734 (1964); P. S. Braterman, R. W. Harrill, and H. D. Kaesz, *ibid.*, **89**, 2851 (1967).

(47) R. V. G. Evans and M. W. Lister, *Trans. Faraday Soc.*, **72**, 1107 (1950).

(48) W. F. Edgell, J. Huff, J. Thomas, H. Lehman, L. Angell, and G. Asato, *J. Amer. Chem. Soc.*, **82**, 1254 (1960); B. A. Frenz and J. A. Ibers, *Inorg. Chem.*, **11**, 1109 (1972).

(49) In a pure CO matrix which has a low substitutional site symmetry (C_2) we observed splitting of some of the spectral lines, probably arising from removal of degeneracy or matrix site symmetry effects. For example M_3 and D_3 (Figure 2C) were badly split in pure CO but less so in CO–Ar matrices (Figure 2B). The evidence suggests that there is not another band under D_3 arising from species M because D_3 has an identical splitting pattern when the concentration of Mn_2 is raised to the point where there is exclusive formation of $Mn_2(CO)_{10}$.

(50) (a) The reluctance of matrix isolated $Mn(CO)_5$ to react further with carbon monoxide (even in pure CO at temperatures as high as 40°K) may be a reflection of a genuine activation and free energy barrier for the reaction

$$Mn(CO)_5 + CO \longrightarrow Mn(CO)_6$$

(which is not really unexpected as $Mn(CO)_6$ would violate the 18-electron formalism), although we cannot eliminate the possibility that the sixth coordination site of $Mn(CO)_5$ is blocked by an isocarbonyl or sideways bonded CO group. The apparent thermal stability of $Mn(CO)_5$ on the other hand must be related to the low temperatures employed and to its extremely low matrix concentrations (less than 1 part in 10^3). Therefore thermal decomposition or interaction with another $Mn(CO)_5$ moiety on deposition or during warm-up experiments is unlikely to occur. (b) Additional support for this assignment stems from the recently reported Re atom CO matrix reaction (E. P. Kündig and G. A. Ozin, *J. Amer. Chem. Soc.*, **96**, 5585 (1974)), which yields spectroscopically pure $Re(CO)_5$ under low Re concentration conditions and mixtures of $Re(CO)_5$–$Re_2(CO)_{10}$ at high Re concentration conditions.

(51) It has been pointed out to us by a referee that there is considerable debate over the ordering of the e and b_2 levels in C_{4v} $M(CO)_5$ species. The ordering of levels has been shown to be quite sensitive to the angle CO_{ax}–M–CO_{eq} (Guenzburger, *et al.*, *Chem. Phys. Lett.*, **14**, 239 (1972)). Thus if the e level lies higher than the b_2, the 15-electron C_{4v} $V(CO)_5$ species will be susceptible to a first-order Jahn–Teller distortion.

(52) Weak bands were observed at 1824 and 1799 cm^{-1} which were not reproducible between different runs and which did not have $^{12}C^{18}O$ counterparts. They are therefore assigned to impurity lines. The weak line at 1850 cm^{-1} is probably $Mn^{12}C^{16}O$, the $Mn^{12}C^{18}O$ line being overlapped by the stronger line of $Mn(^{12}C^{16}O)(^{12}C^{16}O)$ at 1809.6 cm^{-1}.

(53) J.J. Turner, private communication.